Analytical and Bioanalytical Chemistry
https://doi.org/10.1007/s00216-018-1425-8

RESEARCH PAPER

An ultrasensitive sensor based on quantitatively modified upconversion particles for trace bisphenol A detection

Qiaofeng Li[1,2] · Jialei Bai[1] · Shuyue Ren[1] · Jiang Wang[1] · Yifei Gao[3] · Shuang Li[1] · Yuan Peng[1] · Baoan Ning[1] · Zhixian Gao[1]

Received: 20 August 2018 / Revised: 28 September 2018 / Accepted: 9 October 2018

Abstract

Bisphenol A (BPA) is one of the endocrine-disrupting chemicals which might cause reproductive and endocrine system diseases, and poses a serious threat to the ecosystem and human health. This paper reports an ultrasensitive sensor for trace BPA detection employing fluorescence resonance energy transfer (FRET) between modified upconversion nanoparticles (UCNPs) and tetramethylrhodamine. To circumvent the problems of low luminous efficiency of FRET and low sensitivity of sensor, the upconversion nanoparticles with very strong fluorescence efficiency were prepared and quantitatively modified. Results showed that the concentrations of amino groups and streptavidin were 43 nmol/mg and 6.12 μg/mg on the surface of the UCNPs, respectively. Under the optimal detection conditions, the peak intensity of UCNPs at 547 nm was linear with the logarithm of the BPA concentration with the detection limit of 0.05 ng/mL. Without complicated pre-processing, the recoveries were in general between 91.0 and 115.0% in tap water, river water, and disposable paper cup water. Therefore, the proposed sensor is suitable for effective sensing of trace BPA in water samples.

Keywords Sensor · Upconversion particles · Quantitative modification · Bisphenol A

Introduction

Bisphenol A (BPA), a typical environmental estrogen, is widely applied to the plastic products such as disposable paper cup, feeding bottles, and water bottles [1]. What's notable is that it can migrate into water and food by leaching from landfills, combustion of domestic waste, and degradation of plastics in the environment [2], causing the issue of public health [3]. Considering the extensive application and toxicological impacts of BPA, Chinese National Standard (GB 5749-2006, Standards for drinking water quality) proposed that the concentration of BPA in drinking water should not exceed 0.01 mg/L. Therefore, the methods for determining trace BPA may prove to be pivotal and highly desired.

Up to now, different analytical technologies have been used for BPA detection, such as high-performance liquid chromatography (HPLC) [4], chromatography and chromatography-mass spectrometry [5], liquid chromatography coupled with mass spectrometry (LC–MS) [6, 7], immunoassay methods [8–10], and colorimetric methods [11]. These instrumental analysis methods exhibit high accuracy, but the major disadvantages are expensive, time-consuming, and requiring well-trained operators. In view of the complex processes of antibodies and the high requirement in detecting conditions, immunoassay methods might lead to unsatisfactory results. In recent years, a novel single-stranded DNA/RNA oligonucleotides (also called aptamer), selected in vitro by systematic

Qiaofeng Li and Jialei Bai contributed equally to this work.

Electronic supplementary material The online version of this article (https://doi.org/10.1007/s00216-018-1425-8) contains supplementary material, which is available to authorized users.

✉ Baoan Ning
ningba@163.com

✉ Zhixian Gao
gaozhx@163.com

[1] Tianjin Key Laboratory of Risk Assessment and Control Technology for Environment and Food Safety, Institute of Environmental and Operational Medicine, Academy of Military Medical Science, Academy of Military Science, Da Li Road 1, Tianjin 300050, China

[2] State Key Laboratory of Food Science and Technology, School of Food Science and Technology, Lihu Road 1800, Wuxi 214122, Jiangsu, China

[3] School of Chemistry, University of New South Wales, Sydney, NSW 2052, Australia

Published online: 03 November 2018

evolution of ligands by exponential enrichment binding (SELEX) was finally proposed [12]. Aptamer can specifically bind to kinds of targets by folding together or forming certain conformations [13]. Especially, the characteristics of cost-effectiveness and the convenience of synthesis render aptamer an ideal sensing element in BPA determination [14, 15]. Since the BPA aptamer was first screened, many related types of research have been reported [16–22]. Among these methods, the electrochemical method takes up a large proportion. While, the fluorescent methods draw close attention thanks to the advantages of easy operation, quick response, and convenient signal transduction [23].

The mechanism of fluorescence resonance energy transfer (FRET) refers to a typical non-radiation energy transfer from donors to receptors based on the interaction of electrical dipole moment [24]. Spectral overlapping and the suitable distance between donors and receptors facilitate the fluorescence resonance energy transfer effective occurrence. Gold nanoclusters, semiconductor quantum dots (QDs), and fluorescent dye such as carboxytetramethylrhodamine (TAMRA) have been extensively reported as luminophores [25–28]. However, high background signals and lack of stable optical signals limited their wide use in detecting some samples at trace levels. To improve this, many reporters' attentions have shifted to the upconversion nanoparticles which can translate near infrared low-energy excitation radiation to higher visible energy emission. Nevertheless, previous studies based on UCNPs and FRET for detecting bisphenol A are rarely involved, not to mention systematic quantification of modified compounds coating on UCNPs [29–31]. What's more, to the best of our knowledge, the sample pre-treatment of the above methods are complex. Thus, an ultrasensitive and simple method based on modified UCNPs and TAMRA-based FRET are likely to be promising for the detection of trace BPA and other environmental estrogens.

Herein, a sensor based on modified upconversion nanoparticles and FRET was developed for sensitive detection of trace BPA in water samples. Through experimental exploration, the prepared UCNPs possess significant fluorescence efficiency with an ultra-thin silicon shell (6 nm), then streptavidin (SA)-modified UCNPs were prepared and upconversion fluorescence probes were formed as soon as UCNPs labeled with biotin-modified BPA aptamer through biotin-SA system. BPA-cDNA was labeled with TAMRA, rendering the FRET phenomenon possible under the special recognition between BPA aptamer and BPA-cDNA. In the presence of different concentrations of BPA, the fluorescence recovery intensity was proportional to the concentration of BPA. It is noteworthy that we implemented a strategy by connecting the aptamer to the UCNP via the biotin-SA system to achieve signal amplification. More importantly, the UCNPs with much more surface-modified amino groups were preferred and quantified. This strategy could maximize the consumption of the saved biological molecules, and achieve the purpose of minimizing the detection limit, thereby improving the detection sensitivity. Based on the above design, a sensitive and convenient approach was well-established for trace BPA detection.

Material and methods

Reagents and materials

$YCl_3 \cdot 7H_2O$, $YbCl_3 \cdot 6H_2O$, and $ErCl_3 \cdot 6H_2O$ (with the purity 99.99%) were obtained from Xiya Chemical Reagent (Shandong, China). Tetrabromo-bisphenol A (TBBPA), 4,4-bisphenol (BP), bisphenol B (BPB), 4,4′-(hexafluoroisopropylidene) diphenol (6F-BPA), and bisphenol C (BPC) were purchased from Yuanye Biotech Company (Shanghai, China). Tetraethoxysilane (TEOS), bisphenol A (BPA), and 3-aminopropyl triethoxysilane (APTES) were purchased from Sigma-Aldrich Co (St. Louis, MO, USA). Millipore Milli-Q ultrapure water (Millipore, Z 18 MΩ cm^{-1}) was prepared in our laboratory. All solvents and chemicals were of reagent quality and used without further purification. Actual water samples were taken from the tap water in our laboratory and Haihe River in Tianjin, China. Disposable paper cups were bought from the local supermarket.

The BPA aptamer and its complementary DNA were synthesized by Sangon Biological Science & Technology (Shanghai, China). The sequences of the oligonucleotides are designed according to reported studies [17]. The detailed sequences are as follows:

- BPA aptamer: 5′-biotin-CCGGT GGGTG GTCAG GTGGG ATAGC GTTCC GCGTA TGGCC CAGCG CATCA CGGGT TCGCA CCA-3′
- BPA complementary DNA (cDNA): 5′-CTGAC CACCC ACCGG-TAMRA-3′

Apparatus

UV-visible absorption spectra of the modified UCNPs were recorded by a TU-1901 spectrometer (Shimadzu, Japan). Millipore Milli-Q ultrapure (18 MΩ cm^{-1}) was used throughout the whole research and obtained from a Millipore Direct-Q®3 system (Merck Millipore, Billerica, MA, USA). Transmission electron microscopy (TEM, JEOL, Japan) with a JEM-100CXII instrument was performed to observe the size and shape of UCNPs. Fourier-transform infrared spectroscopy (FTIR) of the modified UCNPs were observed via a Bio-Rad FTS6000 Fourier-transform infrared spectrometer (FTIR spectrometer) using the KBr method. The upconversion luminescence spectra were collected by an F-4500 fluorescence

spectrophotometer (Hitachi, Japan) with an external 980-nm laser (Beijing Hi-Tech Optoelectronic, China).

Synthesis and modification of $NaYF_4$: Yb, Er UCNPs

In this study, the UCNPs were synthesized according to related literature [32] and compared under different experimental conditions, such as the molar ratio of $LnCl_3$, maximum temperature, and incubation time. At last, the group with the highest luminous intensity was chosen. The final UCNPs used in this experiment were prepared as follows: $YCl_3 \cdot 7H_2O$, $YbCl_3 \cdot 6H_2O$, and $ErCl_3 \cdot 6H_2O$ (molar ratios, 78% Y:20% Yb:2% Er) were dissolved with 10 mL oleic acid and 35 mL 1-octadecene under constant stirring in a 100-mL flask. Then, it was heated to 160 °C and kept for 15 min to form a homogeneous solution, cooled down to room temperature. Twenty milliliters of a methanol solution containing 0.20 g NaOH and 0.35 g NH_4F was added dropwise into the flask, and the reaction continued for 30 min with vigorous stirring. The mixture was degassed at 100 °C for removing water vapor and methanol. Then, the remaining solution was heated to 320 °C quickly under the nitrogen atmosphere with a retention time of 1 h.

The precipitates were obtained by centrifugation, washed with ethanol for several times, then dried under vacuum at 60 °C for 12 h. Amino-functionalized UCNPs were prepared through the Stöber-based method [33] with minor alteration. Typically, 150 mg of $NaYF_4$: Yb, Er UCNPs was dispersed in 95 mL of alcohol by ultrasonication for 30 min. Then, 3.8 mL of ammonium hydroxide, 30 mL of water, and 90 μL of TEOS were added to the suspension. After the reaction system was sustained at 40 °C under vigorous agitation for 4 h, 300 μL of APTES was added dropwise into the above mixture and the mixture was kept for 6 h. Finally, amino-modified UCNPs were formed and collected by centrifugation, washed with ethanol, and dried at 60 °C for 12 h.

Quantitative modification of UCNPs and fluorescence probe preparation

The connection amount of amino groups and SA quantification coated on the surface of UCNPs were explored cause it might have much more subsequent attachment of biomolecules if much more surface-modified UCNPs existed. The amount of amino groups on the surface of nanoparticles was determined as shown in Fig. S5 (see Electronic Supplementary Material, ESM) and the main experimental steps for SA quantification were referenced to previous research [34]. Firstly, before the quantitative determination, a standard curve was drawn according to the relationship between different concentrations of SA and the characteristic absorption peak of the protein at 282-nm wavelength before and after the SA reaction using a UV-Vis spectrophotometer. Next, 5 mg amino-functionalized UCNPs was dispersed in 2.5 mL of 0.01 M PBS by ultrasonication for at least 15 min, and then 0.63 mL of 25% glutaraldehyde was added and the mixture was shaken gently on a shaking table for 2 h at room temperature. The resultants were separated by centrifugation (10,000 rpm, 10 min) and were washed with PBS for three times to remove redundant glutaraldehyde. The above nanoparticles were redispersed in 0.01 M PBS, then several concentrations of SA were added to the solution and the mixture was shaken slowly for 12 h at 25 °C. Afterwards, the SA-modified UCNPs were centrifuged, washed, and suspended in 2.5 mL of 0.01 M PBS. The first supernatant was used to quantify the connected SA with reference to the standard curve.

Prior to fluorescence probe preparation, the BPA aptamer was pre-treated to ensure the better combination with the target. After dissolution, the aptamer was heated at 95 °C for 5 min, placed in ice water immediately to reduce the effect of nucleic acid secondary structure on the experiment. Next, a certain amount of BPA aptamer was added to 0.5 mg/mL of SA-modified UCNPs at 37 °C for 1 h under vertical mixing. After final centrifugation, the products were washed for three times with PBS and stored at 4 °C before use.

Assay protocol and sample preparation

After the upconversion, fluorescence probe was obtained, a total 500 μL reaction system of the probe and the optimized BPA-cDNA in buffer were incubated at 37 °C for 40 min. After that, the products were separated by centrifugation and resuspended in a buffer, thus BPA probe-cDNA was obtained. After that, 100 μL of BPA standard solutions of various concentrations was added into the reaction system and further incubated at 37 °C for 1 h. After being separated and washed three times, the final mixture was determined with a 980-nm excitation laser to get the luminescence intensity.

Actual water samples used in this work were taken from the tap water in our laboratory, Haihe River in Tianjin, China, and water in disposable paper cups. Considering BPA may dissolve from disposable paper cups at high temperature, the disposable paper cups were placed in 150 mL tap water at 100 °C for 30 min. Then, three kinds of water were not subjected to other complex pre-treatment except filtration by 0.22-μm filter twice.

Results and discussion

Design strategy for this method

The schematic of detection for BPA is shown in Fig. 1. In brief, UCNPs modified with SA are linked to BPA aptamer by the biotin-SA system, subsequently hybridized with the BPA-cDNA; thus, the fluorescence resonance energy transfer occurs between UCNPs and TAMRA. Spectral overlap between UCNPs fluorescence and TAMRA absorption can be seen in Fig. 2. The nanocomposites are formed; witness the minimal

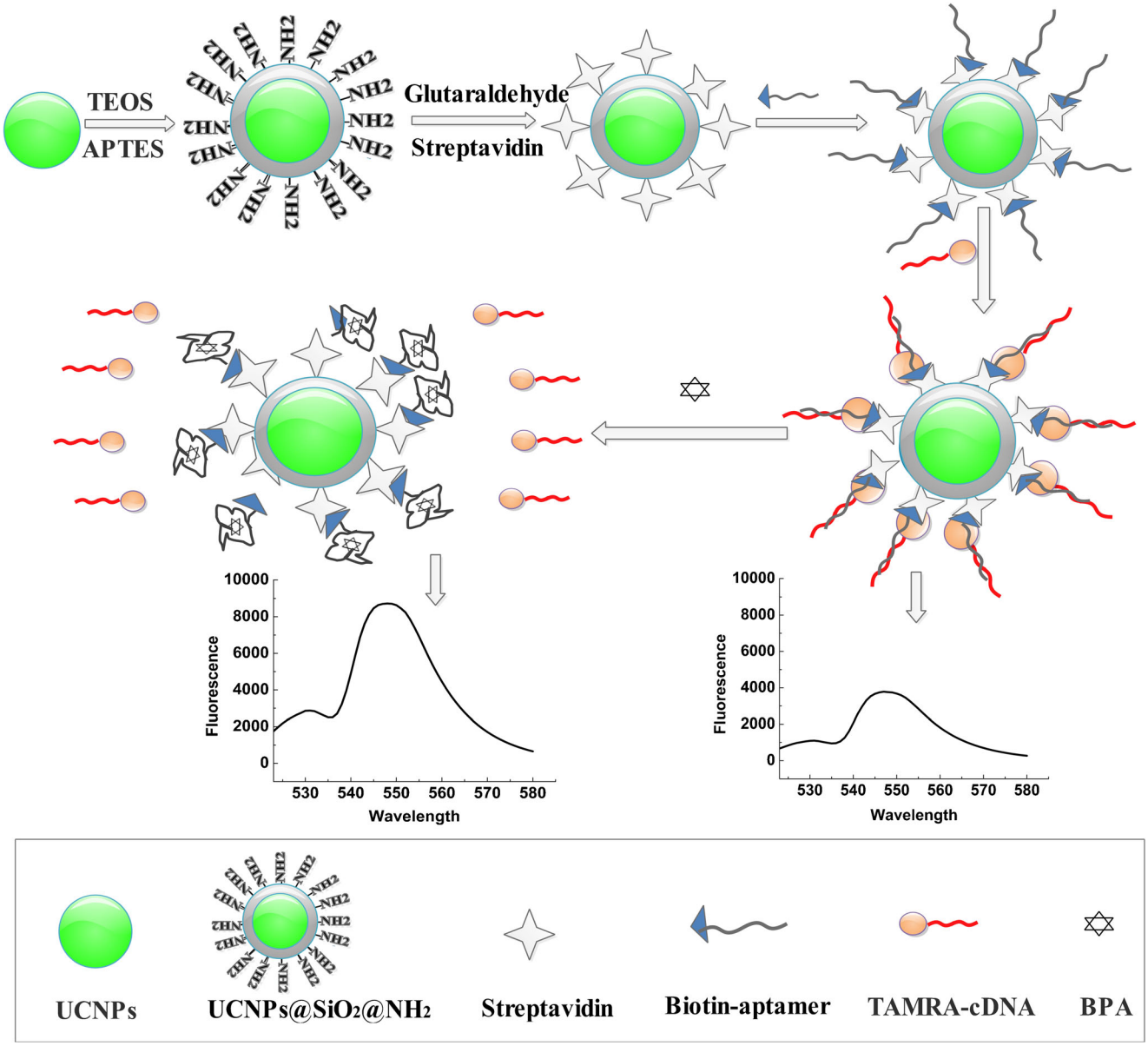

Fig. 1 Schematic illustration for BPA detection

luminescence intensity when the system is excited at 980 nm. In the presence of BPA, the aptamer prefers to bind with BPA which causes the dissociation of some BPA-cDNA and leads to the recovery of fluorescence intensity. As a result, the highly specific and sensitive fluorescence detection of BPA is established and the fluorescence intensity is linearly correlated to the logarithm of the BPA concentration in the sensing system.

Synthesis and characterization

It is found that the molar ratio of lanthanides, incubation temperature, and time had great influence on the size and shape of particles during the synthesis of UCNPs. Therefore, after adjusting the reaction conditions (see ESM Fig. S1 and Table S1), the UCNPs with the highest luminescence efficiency were prepared and chosen by comparing the fluorescence intensity of bare UCNPs and silicon-coated UCNPs (ESM Fig. S2). It is remarkable that UCNPs coated with a silicon shell still exhibit a higher luminescence efficiency and ensure cross-linking of more biomolecules. The TEM images of UCNPs for this research before and after modification are shown in Fig. 3(A) which is from group (C) Fig. S1 (see ESM). The average diameter of UCNPs is 73 nm. After modification, UCNPs increases to approximately 85 nm because of a 6-nm-thick silica layer. Meanwhile, dynamic light scattering was performed to characterize the UCNPs. The average diameters of UCNPs and amino-functionalized UCNPs are measured to be 73 ± 0.5 nm and 85 ± 0.6 nm, respectively (ESM Fig. S3). Moreover, the UCNPs before and after modification were dispersed in water, respectively. Furthermore, the photographs of two groups of UCNPs were taken under natural

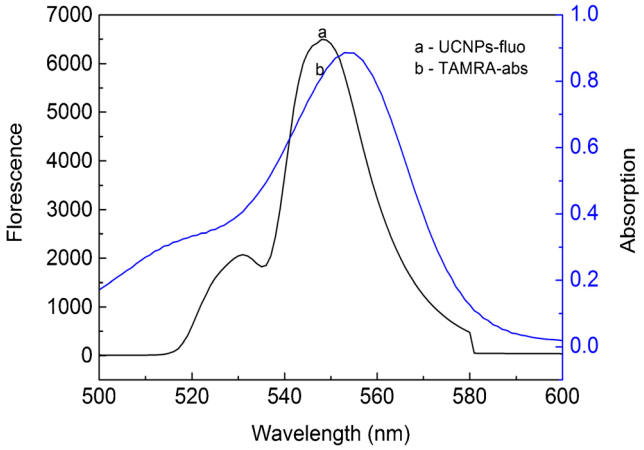

Fig. 2 Spectral overlap between UCNP fluorescence and TAMRA absorption. The absorption spectra of TAMRA (with the maximum absorption wavelength at 553 nm) and the emission spectrum of UCNPs (with the maximum emission wavelength at 547 nm) have a certain overlap which can produce efficient FRET between them under specific conditions

light and 980-nm laser illumination (ESM Fig. S4). Results reveal that the solubility of the UCNPs has changed, indicating the successful surface modification of the UCNPs. The UCNPs emit green fluorescence under 980-nm laser illumination, but there is no significant difference between the two groups of the UCNPs. The phenomenon above indicates the UCNPs still have a strong fluorescence intensity after modification.

To confirm the SA-modified UCNPs, FTIR spectrum was used for characterization. As can be seen in Fig. 3(B), the bands at 2926 cm^{-1} and 2854 cm^{-1} are the asymmetric and symmetric stretching vibrations of a methylene group (-CH2-), respectively, caused by the long-chain alkyl from oleic acid molecules. In addition, the two peaks at 1562 cm^{-1} and 1463 cm^{-1} are assigned to the asymmetric and symmetric stretching vibrations of the carboxylic group (COO-). It confirms that OA-UCNPs have been formed (red line). After silica and SA modification, the symmetric stretching vibration of the silicon-oxygen bond (Si-O) can be found at 1091 cm^{-1}. Meanwhile, the bands at 1650 cm^{-1} and 1535 cm^{-1} appear which belong to the stretching and bending vibrations of an amide group (-CONH-), indicating that the amino-modified UCNPs is successfully formed (black line).

The standard curve of the amino-group quantification of the UCNPs' surface was made (ESM Fig. S5), from which we could calculate each milligram of UCNPs coupled with 43 nmol amino group. The optimal concentration of SA was studied after the amino-functionalized UCNPs conjugated to SA successfully. The conjugation of the SA and amino-functionalized UCNPs was examined by UV-Vis absorption spectroscopy. Figure 4(A) showed the calibration curve of the absorbance versus different concentrations of SA. The distinct decrease of the absorption maximum at 280 nm of the SA concentration in the supernatant before and after the cross-linking reaction suggests that SA is successfully conjugated to amino-modified UCNPs. The optimal concentration of SA is obtained by comparing the absorption decrease between different concentrations of SA which can be seen in Fig. S6 (see ESM). The results show that 0.04 mg/mL of SA exhibits maximum reduction of absorbance. According to the calibration curve of the absorbance versus different concentrations of SA, each milligram of UCNPs could be coupled with 6.12 μg SA.

The nanoparticles were modified in multiple steps, there might be a small amount of other substances in the system. Therefore, we further explored the fluorescence intensity of nanoparticles in different states to analyze whether BPA aptamer was successfully coupled to SA-functionalized UCNPs and cDNA. Figure 4(B) shows the different fluorescence intensities in the system. The fluorescence intensity of UCNPs is the highest, while the others show a slight decrease, but once BPA-aptamer-modified UCNPs and BPA-cDNA are coexisting, the fluorescence intensity will decrease significantly due to the FRET between UCNPs and TAMRA, which indirectly proves the success of coupling BPA aptamer with SA-functionalized UCNPs. The conjugation of BPA aptamer and SA-functionalized UCNPs was determined by a specific adsorption experiment.

Optimization of detection conditions

The fluorescence parameters have a direct influence on the fluorescence intensity of UCNPs: the detection results would be more accurate by optimizing the current intensity and slit width

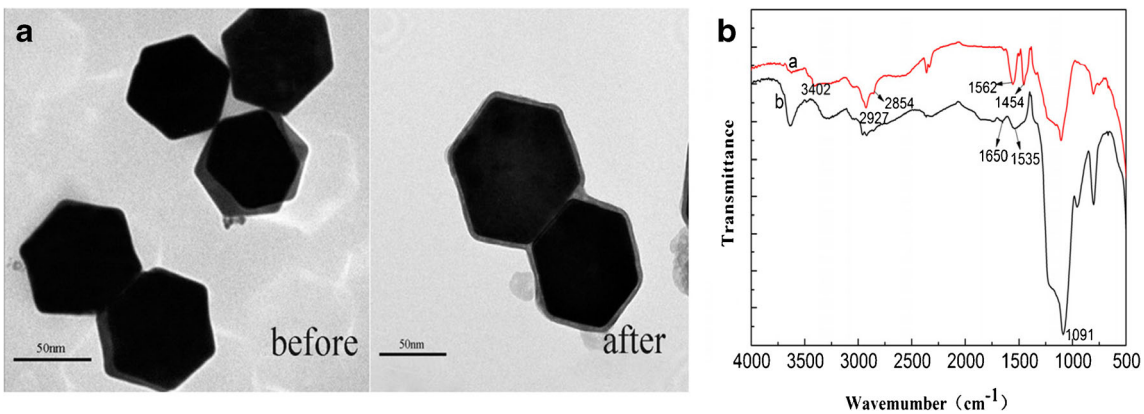

Fig. 3 (A) TEM images of UCNPs before and after modification. (B) FTIR spectra of bare UCNPs (red line) and modification UCNPs (black line)

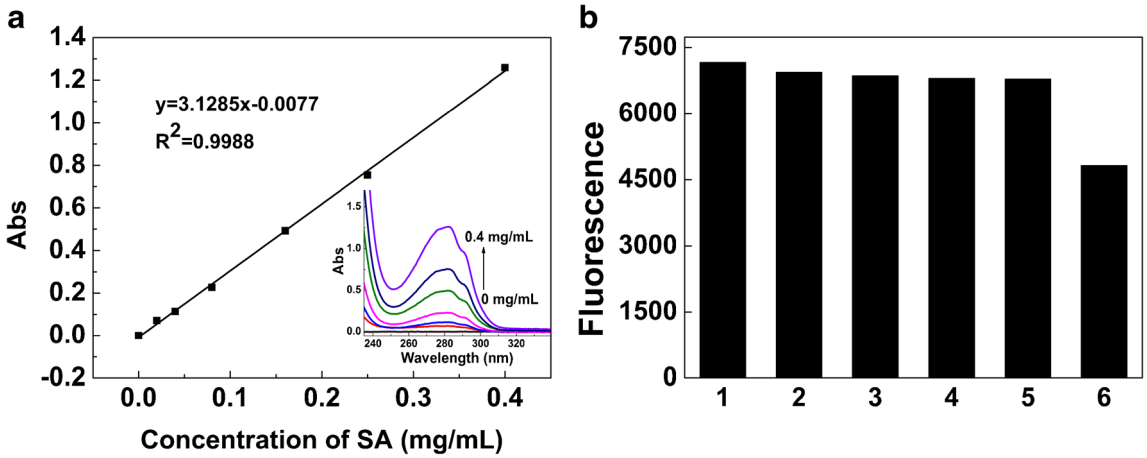

Fig. 4 (A) Calibration curve of the absorbance versus different concentrations of SA. (B) Fluorescence intensity at 547 nm of nanoparticles in different states through specific adsorption experiment (1, UCNPs 2, UCNPs@SiO_2@NH_2 3, UCNPs@SiO_2@SA 4, UCNPs@SiO_2@SA + BPA-aptamer 5, UCNPs@SiO_2@SA + cDNA 6, UCNPs@SiO_2@SA + BPA aptamer + cDNA)

parameters. The changes of parameters have a significant effect on the fluorescence quenching intensity (△F) which can be seen in Fig. 5(A). The more intensity quenched, the wider detection range of BPA is, but the most quenched was discarded in case of great error because it exceeded the instrument range. Therefore, the fluorescence parameters are chosen as follows: the current intensity (*I*), 0.35 A; slit width of excitation luminescence (Ex) and emission luminescence (Em), 2.5 nm and 5.0 nm.

We optimized the type and pH of several buffers as different buffer solutions might seriously impact the detection results. Figure 5(B) shows that the first buffer contributes to the maximum quenching. The reason for this is probably that the appropriate concentrations of sodium and magnesium ions are likely to reduce the Debye length caused by the negative charge of the DNA phosphate backbone, thereby reducing the hybridization resistance and achieving the purpose of more efficient binding of the reactants [35, 36]. According to the information I have, aptamers and its complementary sequences are easier to combine in alkaline solution. Based on the principle of simplicity and practicability, we roughly selected three concentrations and found that the pH 7.6 works best (ESM Fig. S7). Thus, for the buffer of 100 mM NaCl + 10 mM $MgCl_2$ + 10 mM PBS, pH 7.6 is used in the subsequent experiments.

The optimal concentration of aptamer would have a significant effect on the detection sensitivity and linear range. Thus, a comparative study was performed to determine the maximum quenching of the nanocomposites. The mixture of 0.5 mg/mL SA-modified UCNPs and different concentrations of biotin-aptamers was shaken slowly at 25 °C for 1 h. After centrifugation and washing, cDNA was added to the system and hybridized at 37 °C for 40 min. As shown in Fig. 5(C), the quenching intensity increases with an increasing concentration of BPA aptamer, and it reaches a maximum with the addition of 6 μM of BPA aptamer. This indicates that too low or too high concentration of BPA aptamer might count against the effect of reaction, thus the optimal concentration of aptamer is determined.

Just as mentioned above, in the presence of BPA, the aptamer prefers to bind with BPA and causes the dissociation of cDNA, leading to the recovery of fluorescence intensity of UCNPs at 547 nm. Hence, a different incubation time of BPA and aptamer were tested. As shown in Fig. 5(D), with an increase in reaction time from 10 to 60 min, the fluorescence recovery intensity gradually increases. It reaches a maximum at 60 min and then a slight decline occurred. Thus, incubation for 60 min is sufficient for this system.

Assay protocol and calibration curve

Based on the optimal conditions, the variation of fluorescence intensity under different concentrations of BPA was studied. The fluorescence spectrum of various luminous intensities obtained in the presence of different concentrations of BPA is shown in Fig. 6. The results show that fluorescence intensity ΔF (ΔF = $F - F_0$, wherein F_0 and F represent the fluorescence intensity in the absence and presence of different concentrations of BPA, respectively) increases linearly with the logarithm of the BPA concentration in the range of 0.1 to 25 ng/mL (R^2 = 0.9938), which is lower than the maximum residue limit (MRL) 10 ng/mL of BPA in drinking water (GB 5749-2006, National Standard for drinking water quality of China). Such a low detection line might be due to the ultrahigh fluorescence efficiency of UCNPs and the specificity of this method.

Specificity evaluation and sample detection

To investigate the specific response of our new approach to BPA over other analogs, the fluorescence intensity of each analog was recorded. In Fig. 7, the results indicate that BPA induces a noticeable fluorescence change at 547 nm; however, its analogs arouse quite low signals. Moreover, considering that foreign cations and anions may have an effect on the

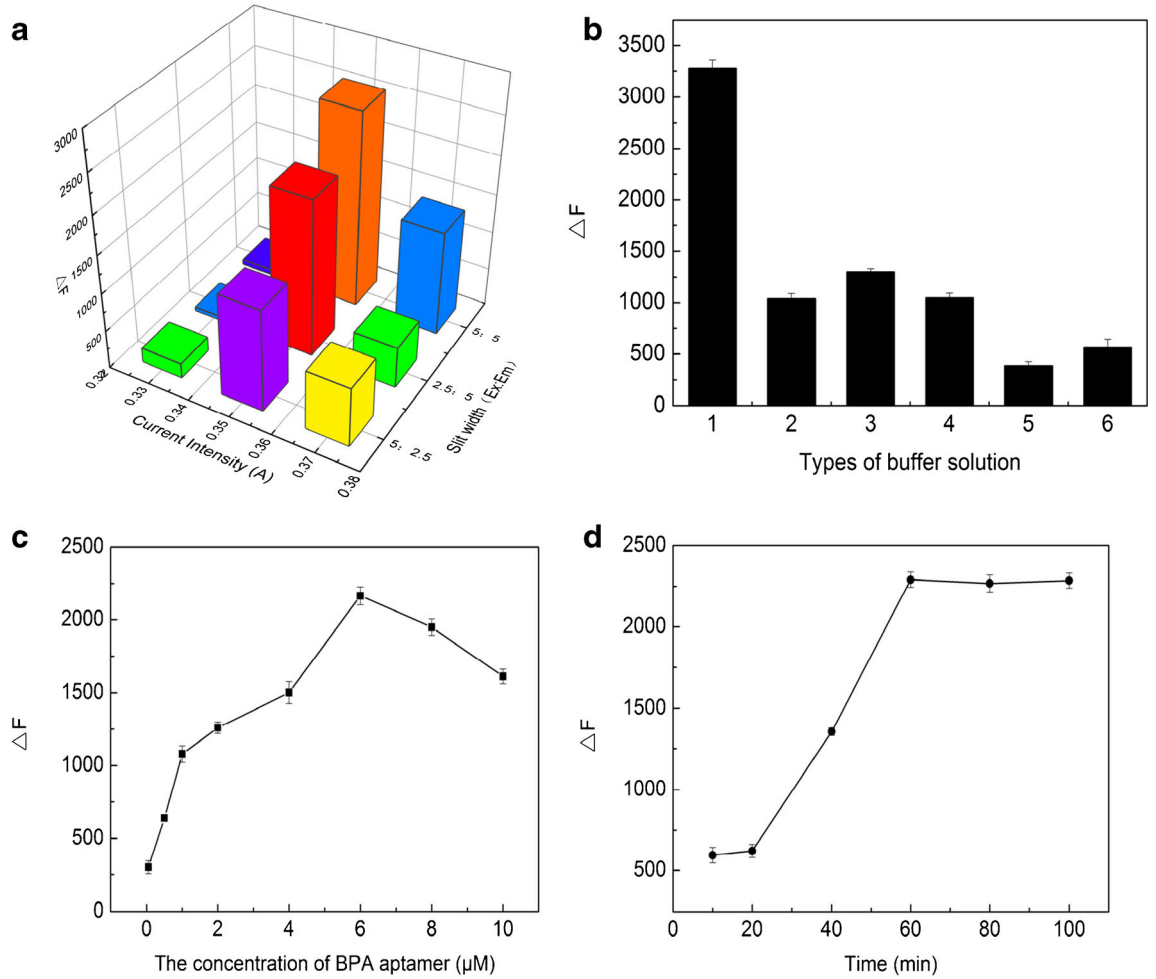

Fig. 5 (A) Optimization of fluorescence parameters. (B) Fluorescence quenching intensity (△F) obtained under various types of buffer (1, 100 mM NaCl + 10 mM $MgCl_2$ + 10 mM PBS, pH 7.6; 2, 0.01 M PBS, pH 7.4; 3, Britton–Robinson buffer, pH 7.5; 4, H_3BO_3-$Na_2B_4O_7$ buffer, pH 7.6; 5, 0.01 M tris-HCl, pH 8.0; 6, 0.05 M PBS, pH 8.0). (C) Fluorescence quenching intensity (△F) obtained using a different concentration of BPA aptamer. (D) Fluorescence quenching intensity (△F) obtained using different incubation times of BPA and aptamer

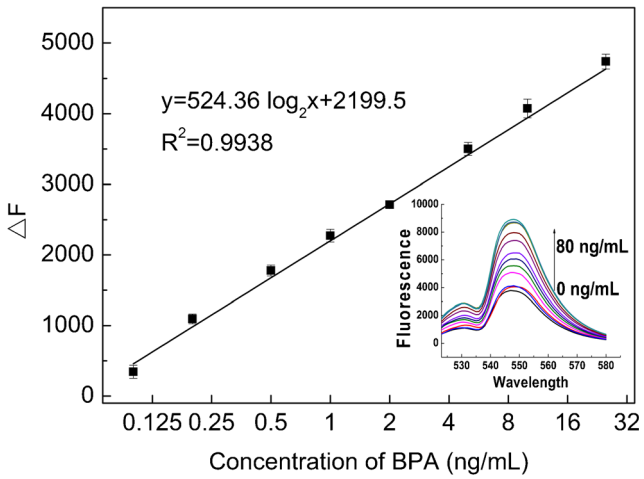

Fig. 6 Calibration curve of the fluorescence intensity ΔF versus different concentrations of BPA by this method. Fluorescence spectrum of sensor at different BPA concentrations from 0 to 80 ng/mL (inset)

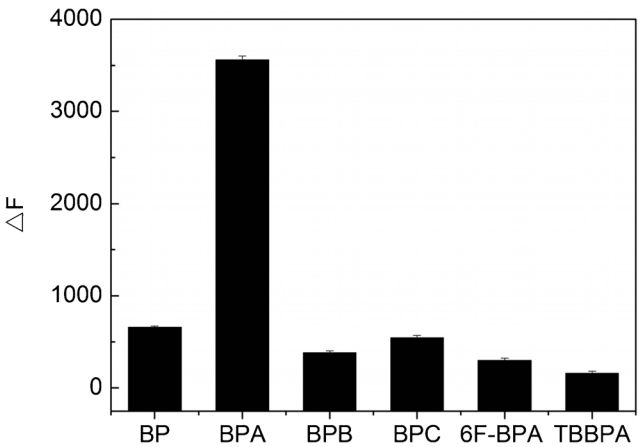

Fig. 7 Specificity of the sensor to BPA by comparison with other analogs, including BP, BPB, BPC, 6F-BPA, and TBBPA

Table 1 Detection results of BPA spiked in water samples via this method ($n = 6$)

Sample	Background (ng/mL)	Added (ng/mL)	Found (ng/mL)	Recovery (%)	RSD (%)
Tap water	0	0.1	0.103	103.0	3.7
	0	5	5.430	108.6	2.8
	0	25	23.102	92.4	2.8
Haihe River	0	0.1	0.091	91.0	2.3
	0	5	5.085	101.7	2.1
	0	25	24.802	99.2	4.5
Disposable paper cup	0.253	0.1	0.368	115.0	7.2
	0.253	5	5.502	105.0	2.6
	0.253	25	25.303	100.2	3.9

experimental results, the different cations and anions (10 times concentration of BPA) were added in the buffer to investigate this conjecture (ESM Fig. S8). The results confirm that this method possesses extraordinary selectivity to BPA. The reason might be that the aptamer mainly binds to the target through the hairpin structure or spatial configuration, and other substances are insufficient to cause conformation change of aptamer, so the influence of the analogs and foreign ions on the detection of actual water sample can be ignored.

Finally, in order to further investigate the application of this method, the spiking known quantity BPA in tap water, water from Haihe River, and water in the disposable paper cup was determined. BPA was detected in the original samples by HPLC. As shown in Table 1, the recoveries are in general between 91.0 and 115.0% and the RSD is below 7.2% which obtained by six independent experiments. A comparison of recovery between this method and other reported methods for BPA is summarized (ESM Table S2). Compared with other methods, the proposed fluorescent method has a wider detection range with the much lower detection limit of 0.05 ng/mL. In addition, the proposed method allows direct detection in real water samples in 2 h with only twice-filtered.

Conclusion

In summary, relying on the quantitatively modified UCNPs, a sensitive sensor was developed for detecting trace BPA in water samples. Compared to other methods, we prepared the high-efficiency luminescent $NaYF_4$: Yb, Er UCNPs and utilized UCNPs and TAMRA making the FRET happen, ensuring a higher fluorescence response and super-duper sensitivity. Through optimizing crucial reaction conditions, the proposed method is superior to other fluorescence methods with the detection limit of 0.05 ng/mL, especially in oversimplified sample pre-treatment. It is reasonable to imagine that this analysis platform possessing the strengths of being highly sensitive, time-saving, simple, and practical provides a useful model for detecting contaminants in water samples.

Funding information This work was supported by the National Natural Science Foundation of China (Grant Nos. 21477162, 81602896, AWS15J006); the Tianjin Research Program of Application Foundation and Advanced Technology (Grant No. 15JCYBJC51200); the National Key Research and Development Program of China (Grant No. 2017YFF0104903) and Natural Science Fund of Tianjin City (Grant No. 17JCQNJC12500).

Compliance with ethical standards

Conflicts of interest The authors declare that they have no competing interest.

References

1. Tang JF, Zhang Y, Gou J, Ma ZL, Li GN, Man YH, et al. Sol-gel prepared Yb3+/Er3+ co-doped RE2O3 (RE = La, Gd, Lu) nanocrystals: structural characterization and temperature-dependent upconversion behavior. J Alloys Compd. 2018;740:229–36. https://doi.org/10.1016/j.jallcom.2018.01.050.
2. Du P, Luo LH, Li WP, Yue QY, Chen HB. Optical temperature sensor based on upconversion emission in Er-doped ferroelectric 0.5Ba(Zr0.2Ti0.8)O-3-0.5(Ba0.7Ca0.3)TiO3 ceramic. Appl Phys Lett. 2014;104(15). https://doi.org/10.1063/1.4871378.
3. Du P, Luo LH, Yu JS. Energy back transfer induced color controllable upconversion emissions in La2MoO6:Er3+/Yb3+ nanocrystals for versatile applications. Part Part Syst Charact. 2018;35(3). https://doi.org/10.1002/ppsc.201700416.
4. Watabe Y, Kondo T, Morita M, Tanaka N, Haginaka J, Hosoya K. Determination of bisphenol A in environmental water at ultra-low level by high-performance liquid chromatography with an effective on-line pretreatment device. J Chromatogr A. 2004;1032(1–2):45–9. https://doi.org/10.1016/j.chroma.2003.11.079.
5. Becerra V, Odermatt J. Detection and quantification of traces of bisphenol A and bisphenol S in paper samples using analytical pyrolysis-GC/MS. Analyst. 2012;137(9):2250–9. https://doi.org/10.1039/c2an15961a.
6. Motoyama A, Suzuki A, Shirota O, Namba R. Direct determination of bisphenol A and nonylphenol in river water by column-switching semi-microcolumn liquid chromatography/electrospray mass spectrometry. Rapid Commun Mass Spectrom. 1999;13(21):2204–8. https://doi.org/10.1002/(sici)1097-0231(19991115)13:21<2204::aid-rcm776>3.0.co;2-9.
7. Zhou X, Kramer JP, Calafat AM, Ye X. Automated on-line column-switching high performance liquid chromatography isotope dilution tandem mass spectrometry method for the quantification of bisphenol A, bisphenol F, bisphenol S, and 11 other phenols in urine. J Chromatogr B Anal Technol Biomed Life Sci. 2014;944:152–6. https://doi.org/10.1016/j.jchromb.2013.11.009.
8. Miao W, Wei B, Yang R, Wu C, Lou D, Jiang W, et al. Highly specific and sensitive detection of bisphenol A in water samples using an enzyme-linked immunosorbent assay employing a novel synthetic antigen. New J Chem. 2014;38(2):669–75. https://doi.org/10.1039/C3NJ01094E.
9. Moreno MJ, D'Arienzo P, Manclus JJ, Montoya A. Development of monoclonal antibody-based immunoassays for the analysis of bisphenol A in canned vegetables. J Environ Sci Health B. 2011;46(6):509–17. https://doi.org/10.1080/03601234.2011.583871.

10. Zhao MP, Li YZ, Guo ZQ, Zhang XX, Chang WB. A new competitive enzyme-linked immunosorbent assay (ELISA) for determination of estrogenic bisphenols. Talanta. 2002;57(6):1205–10.
11. Liang X, Wang H, Wang H, Pei G. Colorimetric detection of bisphenol A using Au-Fe alloy nanoparticle aggregation. Anal Methods. 2015;7(9):3952–7. https://doi.org/10.1039/C5AY00090D.
12. Ellington AD, Szostak JW. In vitro selection of RNA molecules that bind specific ligands. Nature. 1990;346(6287):818–22. https://doi.org/10.1038/346818a0.
13. Tuerk C, Gold L. Systematic evolution of ligands by exponential enrichment: RNA ligands to bacteriophage T4 DNA polymerase. Science (New York, NY). 1990;249(4968):505–10.
14. Tombelli S, Minunni M, Mascini M. Analytical applications of aptamers. Biosens Bioelectron. 2005;20(12):2424–34. https://doi.org/10.1016/j.bios.2004.11.006.
15. Xing H, Hwang K, Li J, Torabi S-F, Lu Y. DNA aptamer technology for personalized medicine. Curr Opin Chem Eng. 2014;4:79–87. https://doi.org/10.1016/j.coche.2014.01.007.
16. Guo X, Wu S, Duan N, Wang Z. Mn(2+)-doped NaYF4:Yb/Er upconversion nanoparticle-based electrochemiluminescent aptasensor for bisphenol A. Anal Bioanal Chem. 2016;408(14):3823–31. https://doi.org/10.1007/s00216-016-9470-7.
17. Jo M, Ahn J-Y, Lee J, Lee S, Hong SW, Yoo J-W, et al. Development of single-stranded DNA aptamers for specific bisphenol A detection. Oligonucleotides. 2011;21(2):85–91. https://doi.org/10.1089/oli.2010.0267.
18. Pan D, Gu Y, Lan H, Sun Y, Gao H. Functional graphene-gold nano-composite fabricated electrochemical biosensor for direct and rapid detection of bisphenol A. Anal Chim Acta. 2015;853:297–302. https://doi.org/10.1016/j.aca.2014.11.004.
19. Xue F, Wu J, Chu H, Mei Z, Ye Y, Liu J, et al. Electrochemical aptasensor for the determination of bisphenol A in drinking water. Microchim Acta. 2013;180(1):109–15. https://doi.org/10.1007/s00604-012-0909-z.
20. Yildirim N, Long F, He M, Shi H-C, Gu AZ. A portable optic fiber aptasensor for sensitive, specific and rapid detection of bisphenol-A in water samples. Environ Sci Process Impacts. 2014;16(6):1379–86. https://doi.org/10.1039/C4EM00046C.
21. Yu P, Liu Y, Zhang X, Zhou J, Xiong E, Li X, et al. A novel electrochemical aptasensor for bisphenol A assay based on triple-signaling strategy. Biosens Bioelectron. 2016;79:22–8. https://doi.org/10.1016/j.bios.2015.12.007.
22. Zhou L, Wang J, Li D, Li Y. An electrochemical aptasensor based on gold nanoparticles dotted graphene modified glassy carbon electrode for label-free detection of bisphenol A in milk samples. Food Chem. 2014;162:34–40. https://doi.org/10.1016/j.foodchem.2014.04.058.
23. Zhong W. Nanomaterials in fluorescence-based biosensing. Anal Bioanal Chem. 2009;394(1):47–59. https://doi.org/10.1007/s00216-009-2643-x.
24. Zhu Y, Cai Y, Xu L, Zheng L, Wang L, Qi B, et al. Building an aptamer/graphene oxide FRET biosensor for one-step detection of bisphenol A. ACS Appl Mater Interfaces. 2015;7(14):7492–6. https://doi.org/10.1021/acsami.5b00199.
25. Kuang R, Kuang X, Pan S, Zheng X, Duan J, Duan Y. Synthesis of cysteamine-coated CdTe quantum dots for the detection of bisphenol A. Microchim Acta. 2010;169(1–2):109–15.
26. Li Y, Xu J, Wang L, Huang Y, Guo J, Cao X, et al. Aptamer-based fluorescent detection of bisphenol A using nonconjugated gold nanoparticles and CdTe quantum dots. Sensors Actuators B Chem. 2016;222:815–22. https://doi.org/10.1016/j.snb.2015.08.130.
27. Li DY, Wang YX, Zhang XR, Yang K, Liu L, Song YL. Optical temperature sensor through infrared excited blue upconversion emission in Tm3+/Yb3+ codoped Y2O3. Opt Commun. 2012;285(7):1925–8. https://doi.org/10.1016/j.optcom.2011.12.075.
28. Peng J, Gao W, Gupta BK, Liu Z, Romero-Aburto R, Ge L, et al. Graphene quantum dots derived from carbon fibers. Nano Lett. 2012;12(2):844–9. https://doi.org/10.1021/nl2038979.
29. Wu S, Duan N, Zhu C, Ma X, Wang M, Wang Z. Magnetic nanobead-based immunoassay for the simultaneous detection of aflatoxin B1 and ochratoxin A using upconversion nanoparticles as multicolor labels. Biosens Bioelectron. 2011;30(1):35–42. https://doi.org/10.1016/j.bios.2011.08.023.
30. Yin M, Wu L, Li Z, Ren J, Qu X. Facile in situ fabrication of graphene-upconversion hybrid materials with amplified electrogenerated chemiluminescence. Nanoscale. 2012;4(2):400–4. https://doi.org/10.1039/C1NR11393C.
31. Wang L, Yan R, Huo Z, Wang L, Zeng J, Bao J, et al. Fluorescence resonant energy transfer biosensor based on upconversion-luminescent nanoparticles. Angew Chem Int Ed Eng. 2005;44(37):6054–7. https://doi.org/10.1002/anie.200501907.
32. Zhang ZLY. An efficient and user-friendly method for the synthesis of hexagonal-phase NaYF4:Yb, Er/Tm nanocrystals with controllable shape and upconversion fluorescence. Nanotechnology. 2008. https://doi.org/10.1088/0957-4484/19/34/345606.
33. Stalder K, Stober W. Haemolytic activity of suspensions of different silica modifications and inert dusts. Nature. 1965;207(4999):874–5.
34. Wu S, Duan N, Ma X, Xia Y, Wang H, Wang Z, et al. Multiplexed fluorescence resonance energy transfer aptasensor between upconversion nanoparticles and graphene oxide for the simultaneous determination of mycotoxins. Anal Chem. 2012;84(14):6263–70. https://doi.org/10.1021/ac301534w.
35. Chu C-H, Sarangadharan I, Regmi A, Chen Y-W, Hsu C-P, Chang W-H, et al. Beyond the Debye length in high ionic strength solution: direct protein detection with field-effect transistors (FETs) in human serum. Sci Rep. 2017;7(1):5256. https://doi.org/10.1038/s41598-017-05426-6.
36. Stern E, Vacic A, Rajan NK, Criscione JM, Park J, Ilic BR, et al. Label-free biomarker detection from whole blood. Nat Nanotechnol. 2009;5:138. https://doi.org/10.1038/nnano.2009.353 https://www.nature.com/articles/nnano.2009.353#supplementary-information.